

Title No. 115-S26

# Truss Model for Shear Strength of Structural Concrete Walls

by Jimmy Chandra, Khatthanam Chanthabouala, and Susanto Teng

Numerous methods for calculating shear strengths of structural walls are available. However, due to the complexity of wall behaviors and possible loading combinations that they may be subjected to, it is quite challenging to derive a method that is reasonably simple but can accommodate various influencing parameters in order to acquire more accurate predictions of wall shear strengths. The authors had earlier tested a series of very-high-strength concrete wall specimens ( $f'_c = 100$  MPa [14,500 psi]) to investigate the influence on shear strength of several parameters, such as: height-to-length ratios, shear (web) reinforcement ratios in the vertical and horizontal directions, as well as the presence of flanges (boundary elements). The conclusions of the authors' experimental study in the light of other research results reported by other researchers will be summarized herein and will be used as a guide for deriving a proposed truss model.

The proposed model is based on modern truss analogy principles (softened truss model, compression field theory) and it has been shown by comparing it with experimental results to be accurate and stable. The design and analysis procedure based on the proposed truss model will also represent an improvement over existing ACI and Eurocode design procedures.

**Keywords:** building codes; high-strength concrete; horizontal reinforcement; shear reinforcement; shear strength; structural walls; truss analogy; vertical reinforcement.

## INTRODUCTION

### General wall behavior

Reinforced concrete (RC) walls are commonly used to carry lateral wind or earthquake loads, as well as to carry vertical (gravity) loads from adjacent floors and transfer beams. The overall height of the wall can be single-story, double-story, or multi-stories up to tall walls. The height-to-length ratio ( $h_w/l_w$ ) can be less than 2.0 for low-rise (squat) walls or much greater than 2.0 for tall walls in taller buildings.

Previous studies<sup>1,2</sup> show that the behavior of structural walls having  $h_w/l_w$  greater than 3.0 is governed mainly by their flexural behavior, those with  $h_w/l_w$  between 2.0 and 3.0 is governed by combined flexural and shear behavior, and those with  $h_w/l_w$  of less than 2.0 is governed more by shear behavior. It is generally understood that flexural behavior of walls can be studied reasonably accurately using normal flexural theory,<sup>3</sup> and the flexural strength of walls can be predicted reasonably accurately also using the normal flexural theory as described in various building codes. The shear behavior of walls, however, is more complex than the flexural behavior, and more research is needed to understand the shear behavior of walls as it is affected by concrete compressive strength ( $f'_c$ ),  $h_w/l_w$ , vertical and horizontal web reinforcement ratios ( $\rho_v$  and  $\rho_h$ ), as well as the presence

of flanges. Therefore, this paper concentrates on the shear behavior, especially at the ultimate limit state.

Note that building code formulas (ACI 318-14<sup>4</sup> and Eurocode 8<sup>5</sup>) for calculating the shear strength of reinforced concrete (RC) walls subjected to seismic loading are mainly empirical and, as such, their applicability may not be as wide as they could be. Based on previous experimental study by the authors,<sup>6</sup> it can be concluded that the ACI 318 neglects the contribution of vertical shear (wall) reinforcement while the Eurocode 8, for walls with  $h_w/l_w$  of 2.0 or greater, considers that the shear strength of walls depends only on the horizontal shear reinforcement. Dowel action in walls with flanges plays a significant role in determining wall shear strengths, and this dowel action has not been treated accurately by building codes. The use of very-high-strength concrete may also introduce inaccuracy in code procedures, as those formulas are not intended for very-high-strength concrete walls. Nevertheless, the authors<sup>6</sup> had also found that ACI 318 has low safety factors for walls with  $f'_c$  of 60 MPa (8700 psi) or lower. Eurocode 8, however, is overly conservative for all cases of concrete strengths. These conditions call for more research and new design procedures for structural walls.

The rational theory for predicting shear strength of RC members was developed based on the classical truss analogy in early 1900s, and since then it has undergone many major developments to arrive at a better accuracy in predicting the shear strength of RC members. For RC walls, which can be categorized as membrane elements, much research has been conducted to predict their shear strengths (refer to Bažant's microplane model,<sup>7</sup> Okamura and Maekawa's stress field formulation,<sup>8</sup> Vecchio and Collins' modified compression field theory,<sup>9</sup> and Hsu's softened truss model<sup>10</sup>). All of these formulations or theories are able to produce complete load-deformation response of given RC membrane elements, shells, or walls. Those theories, however, require the use of a nonlinear finite element procedure in their implementation. Therefore, to take advantage of their superior theoretical derivations for engineering design purposes, some simplifications are needed.

*ACI Structural Journal*, V. 115, No. 2, March 2018.

MS No. S-2015-425.R2, doi: 10.14359/51701129, was received May 29, 2017, and reviewed under Institute publication policies. Copyright © 2018, American Concrete Institute. All rights reserved, including the making of copies unless permission is obtained from the copyright proprietors. Pertinent discussion including author's closure, if any, will be published ten months from this journal's date if the discussion is received within four months of the paper's print publication.

The proposed truss model is intended to address some of those issues in building code formulas and to improve the predictions of RC wall shear strengths.

### RESEARCH SIGNIFICANCE

Based on the authors' test data on very-high-strength concrete walls as well as data from literature, the authors attempt to introduce a new method for calculating the shear strength of RC walls. The method is based on modern field truss analogy principles such as the softened truss model and the compression field theory. The new proposed method is intended for the ultimate limit state and has been shown to be reasonably accurate and reliable. The authors expect that this research can highlight useful concepts that may help our understanding of structural wall behavior.

### CODE AND OTHER METHODS

The ACI 318 and the Eurocode 8 are two reference building codes that are adopted in many countries, including Singapore. As such, those two building codes and two more proposed methods by other researchers<sup>11,12</sup> are reviewed briefly below and their performance will then be compared with available experimental results, including the authors' test results.

#### ACI 318-14

According to ACI 318-14,<sup>4</sup> the nominal shear strength ( $V_n$ ) of RC walls subjected to seismic loading can be calculated as follows

$$V_n = A_{cv} (\alpha_c \lambda \sqrt{f'_c} + \rho_t f_y) \quad (\text{ACI 318-14 Eq. (18.10.4.1)})$$

ACI 318-14 also states that the value of  $V_n$  shall not exceed  $0.83A_{cv}\sqrt{f'_c}$  (in Newtons). Even though ACI 318-14 does not directly consider the contribution of vertical shear reinforcement to shear strength, it does require that structural walls be provided with vertical shear reinforcement of the amount that depends on  $h_w/l_w$ .

#### Eurocode 8 (EN 1998-1:2004)

According to Eurocode 8,<sup>5</sup> or EC8, the ultimate shear strength of RC walls subjected to earthquake loads can be taken as the smaller of the shear strengths or shear resistance calculated from two shear failures of the wall web: 1) diagonal compression failure ( $V_{Rd,max}$ ); and 2) diagonal tension failures, either  $V_{Rd,s}$  or  $V_{Rd}$  (refer to the following).

*Diagonal compression failure of the web due to shear*—For the case of diagonal compression failure, the shear strength (resistance) is given by  $V_{Rd,max}$

$$V_{Rd,max} = \alpha_{cw} b_w z v_1 f_{cd} / (\cot\theta + \tan\theta) \quad (1a)$$

where the recommended value of  $\alpha_{cw}$  is as follows

$$1.0 \text{ for non-prestressed structures} \quad (1b)$$

$$(1.0 + \sigma_{cp}/f_{cd}) \text{ for } 0 < \sigma_{cp} \leq 0.25f_{cd} \quad (1c)$$

$$1.25 \text{ for } 0.25f_{cd} < \sigma_{cp} \leq 0.5f_{cd} \quad (1d)$$

$$2.5(1.0 - \sigma_{cp}/f_{cd}) \text{ for } 0.5f_{cd} < \sigma_{cp} < 1.0f_{cd} \quad (1e)$$

The recommended value for  $v_1$  is  $0.6[1.0 - f_{ck}/250]$  ( $f_{ck}$  in MPa).

EC8 recommends that the values of  $\cot\theta$  and  $\tan\theta$  are taken as 1.0.

*Diagonal tension failure of the web due to shear, either  $V_{Rd,s}$  or  $V_{Rd}$* —If  $\alpha_s = M_{Ed}/(V_{Ed}l_w) \geq 2.0$ , where  $M_{Ed}$  is the design bending moment at the base of the wall and  $V_{Ed}$  is the design shear force, then the shear strength (resistance) is given by  $V_{Rd,s}$

$$V_{Rd,s} = \frac{A_{sv}}{s} z f_{ywd} \cot\theta \quad (2)$$

If  $\alpha_s = M_{Ed}/(V_{Ed}l_w) < 2.0$ , the shear strength (resistance) is given by  $V_{Rd}$

$$V_{Rd} = V_{Rd,c} + 0.75\rho_h f_{yd,h} b_{wo} \alpha_s l_w \quad (3)$$

#### Hwang-Lee's method

Hwang and Lee<sup>11</sup> proposed a method based on the strut-and-tie model for calculating the shear strength of RC walls. In their model, the applied external forces were assumed to be resisted by combination of concrete compression struts and steel tension ties, as shown in Fig. 1. There are three load paths—that is, diagonal, vertical, and horizontal components. The diagonal compression force acting on nodal zone,  $C_{d,n}$  is calculated from the three components according to their relative stiffness ( $R_d$ ,  $R_v$ , and  $R_h$ ). Then, the shear capacity of RC wall is determined by the nominal capacity of the nodal zone as given by Eq. (4a). The nominal shear strength of an RC wall can be calculated as the horizontal component of the diagonal compression force that is corresponding to the nominal capacity of the nodal zone. The softening behavior of cracked concrete has also been accounted for in their method. Thus, the model is called softened strut-and-tie model

$$C_{d,n} = K \zeta f'_c A_{str} \quad (4a)$$

where  $K$  is the strut-and-tie index, which is defined as follows

$$K = \frac{-D + \frac{F_h}{\cos\theta} + \frac{F_v}{\sin\theta}}{-D + \frac{F_h}{\cos\theta} \left(1 - \frac{\sin^2\theta}{2}\right) + \frac{F_v}{\sin\theta} \left(1 - \frac{\cos^2\theta}{2}\right)} \geq 1.00 \quad (4b)$$

The variable  $\zeta$  is the softening coefficient of cracked diagonal concrete strut, which is approximated as  $(3.35/\sqrt{f'_c})$  and should not be taken more than 0.52.

#### Gupta and Rangan's method

Another analytical method considered herein for calculating the shear strength of RC walls is the one developed by Gupta and Rangan.<sup>12</sup> They used the Modified Compression

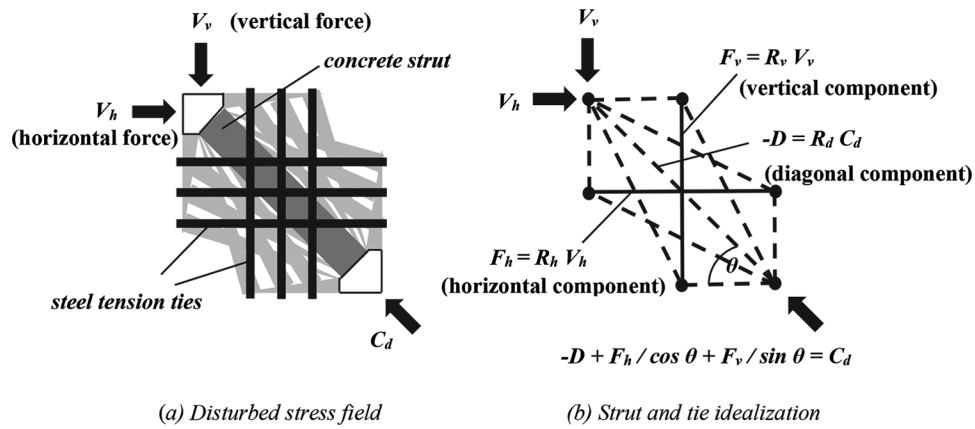


Fig. 1—Strut-and-tie mechanisms proposed by Hwang and Lee.<sup>11</sup>

Field Theory<sup>9</sup> as the basis for their model. They assumed that the shear force due to external lateral load was primarily resisted by wall panel and the effect of bending stresses on the shear behavior of the panel was negligible. The shear stress on the wall panel was assumed to be uniform and acted over an effective shear area, which was taken as wall thickness ( $t_w$ ) multiplied by the effective depth of the wall ( $d_w$ ). In the stress analysis, they considered equilibrium conditions, strain compatibility, and stress-strain relationships of concrete and steel. They also took into account the softening behavior of cracked concrete as proposed by Collins et al.<sup>13</sup> One of the main assumptions in their model is the value of the strut angle that is assumed to be constant and depended upon the effective depth of the wall ( $d_w$ ) and wall height ( $h_w$ ). The strut angle is given by Eq. (5). However, the strut angle ( $\alpha$ ), as calculated by Eq. (5), does not need to be taken larger than the value calculated for the condition when transverse strain  $\epsilon_t = 0$  and does not need to be taken smaller than the value calculated for the condition when transverse stress ( $\sigma_t$ ) = 0. In other words, these values become lower and upper limits for the strut angle ( $\alpha$ ). This equation provides the necessary condition to solve the equilibrium and compatibility conditions at each analysis stage. The procedure is started with small strain value and it is repeated with certain strain increment until the force-displacement relationship of the RC wall is obtained. The nominal shear strength of RC wall is then taken as the maximum shear force obtained from the force-displacement relationship of the RC wall

$$\tan \alpha = \frac{d_w}{h_w} \quad (5)$$

### NEW PROPOSED METHOD

The minimum requirement for a design procedure is the fulfillment of the equilibrium conditions and applicable materials laws. The purpose of the authors' proposed truss model is to estimate shear strength at ultimate stage.

### Equilibrium conditions

Consider a typical RC wall panel as shown in Fig. 2(a). The applied external shear force ( $V$ ) and the applied external axial force ( $P$ ) are assumed to be distributed uniformly

throughout the wall panel by means of a rigid top beam or slab. As the external shear force  $V$  increases in magnitude, diagonal cracks occur in the wall panel, forming a series of concrete diagonal struts with a certain angle ( $\theta$ ) to the horizontal axis. At ultimate stage, as shown in Fig. 2(b), the stresses in wall panel are a summation of stress in concrete struts and stress in web reinforcement. In this model, the principal stress directions of the concrete are assumed to coincide with the directions of cracks, and the steel bars in the wall panel are assumed to take only axial stresses, neglecting dowel action of web reinforcement.

Note that in addition to the natural coordinate system in the horizontal and vertical directions, or the v-h axes, another coordinate system, r-d, is needed to describe the principal stress directions. To obtain the three stress components— $\sigma_v$ ,  $\sigma_h$ , and  $\tau_{vh}$ —that represent the applied stresses in the vertical and horizontal directions (v-h axes) in terms of stresses in the r-d directions, consider the wedge A-o-p in Fig. 2(c). This wedge is a cutout of the rectangular block ABCD in Fig. 2(b) and is also an enlarged portion of the RC wall panel of Fig. 2(a). Let the thickness of the RC wall panel be one unit and the length of the side o-p of wedge A-o-p be one unit as well. Hence, the area of the side o-p is one-unit area and the areas of A-o and A-p sides become  $\cos\theta$  and  $\sin\theta$ , respectively. Figure 2(c) also shows a diagram of idealized average stresses acting on wedge A-o-p. By taking the summation of average forces (stress multiplied by area) in the vertical direction, stress component in the vertical direction,  $\sigma_v$ , can be obtained as given by Eq. (6). Similarly, Fig. 2(d) shows a diagram of idealized average stresses acting on wedge B-m-n. Stress component in the horizontal direction,  $\sigma_h$ , can be obtained from equilibrium of forces in the horizontal direction, and this is presented in Eq. (7). To obtain shear stress  $\tau_{vh}$ , equilibrium in the horizontal direction of forces acting on wedge A-o-p in Fig. 2(c) can be used. The shear stress  $\tau_{vh}$  in this case is given in Eq. (8). Hence, the three average stresses in the v-h axes of the RC wall panel in terms of the principal stresses  $\sigma_d$  and  $\sigma_r$ , with  $\tau_{rd}$  being zero or vanished in the principal directions, are represented by Eq. (6) to (8), as shown below.

Average stress equilibriums in wall panel

$$\sigma_v = \sigma_d \sin^2 \theta + \sigma_r \cos^2 \theta + \rho_v f_v \quad (6)$$

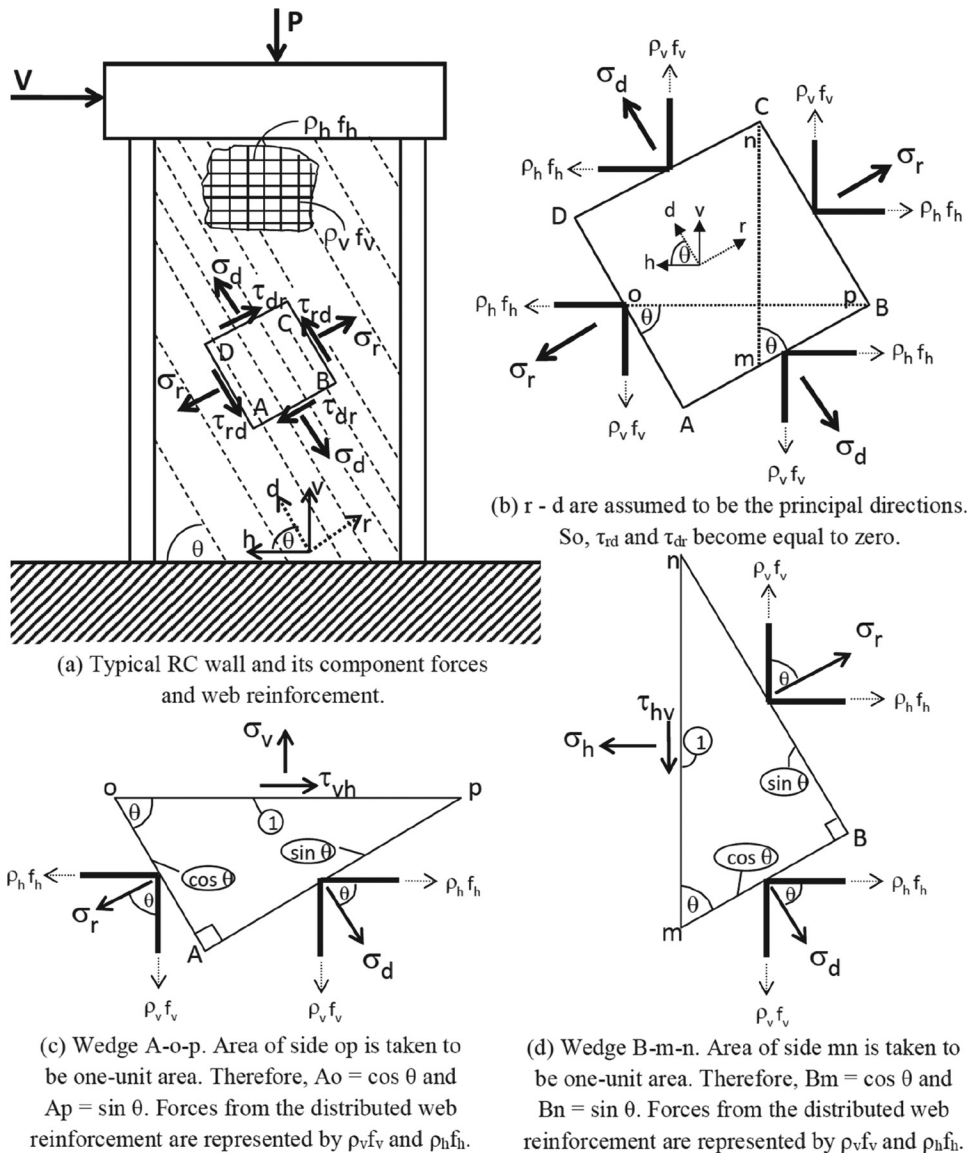


Fig. 2—State of stresses in a typical RC wall panel.

$$\sigma_h = \sigma_d \cos^2 \theta + \sigma_r \sin^2 \theta + \rho_h f_h \quad (7)$$

$$\tau_{vh} = (\sigma_r - \sigma_d) \sin \theta \cos \theta \quad (8)$$

where  $\sigma_v$  is applied normal stress in vertical direction (axis), positive for tension;  $\sigma_h$  is applied normal stress in horizontal direction (axis), positive for tension;  $\sigma_d$  is principal stress of concrete in  $d$ -axis, positive for tension;  $\sigma_r$  is principal stress of concrete in  $r$ -axis, positive for tension;  $\tau_{vh}$  is average shear stress in  $v$ - $h$  coordinate system and is due to shear force acting on the wall;  $\rho_v$  is average vertical web reinforcement ratio;  $\rho_h$  is average horizontal web reinforcement ratio;  $f_v$  is average stress in the vertical web reinforcement;  $f_h$  is average stress in the horizontal web reinforcement; and  $\theta$  is angle of diagonal concrete strut ( $d$ -axis) with respect to horizontal axis at ultimate stage.

### Conditions at ultimate load stage

The overall shear strength of an RC wall is governed by either web reinforcement yielding or diagonal concrete strut

crushing. The procedure to calculate the shear strength can be described as follows.

By imposing equilibrium in the vertical and horizontal directions of the wall, Eq. (6) and (7) can be combined to become Eq. (9). Equation (9) can also be rearranged into Eq. (10)

$$\sigma_v + \sigma_h = \sigma_d + \sigma_r + \rho_v f_v + \rho_h f_h \quad (9)$$

$$-\sigma_d = -\sigma_v - \sigma_h + \sigma_r + \rho_v f_v + \rho_h f_h \quad (10)$$

At ultimate load stage, either the diagonal concrete struts or web reinforcements will reach their individual capacities. Therefore, it is necessary to know which failure mode governs the overall shear strength of the RC wall. The necessary steps start with Eq. (10) and are as follows.

Certain quantities such as  $\sigma_v$ ,  $\sigma_h$ , and  $\sigma_r$  can be calculated easily and then substituted into Eq. (10). The variable  $\sigma_v$  is the applied normal stress in the vertical direction caused by the applied axial force ( $= P/A_g$ ) and it is positive for tension and negative for compression. The  $\sigma_h$  is mostly zero in a

typical RC wall. The variable  $\sigma_r$ , which is the principal tensile stress in concrete in the r-axis can be replaced by the assumed average residual tensile stress in cracked diagonal concrete strut. This tensile stress is also to take into account the stiffening effect of steel bars in concrete in tension. Normally,  $\sigma_r$  is defined as a function of the principal strain of the concrete in the r-axis ( $\epsilon_r$ ).<sup>14,15</sup> However, in this proposed model, which is intended for the ultimate condition only, the average residual tensile stress in cracked diagonal concrete strut ( $\sigma_r$ ) is estimated as 2% of concrete cylinder compressive strength ( $0.02f'_c$ ), as shown in Fig. 3. This assumption is based on experimental data on stress-strain behavior of concrete in tension<sup>16-18</sup>; that is, the residual tensile strength of concrete is about 20% of its peak tensile strength. Hence, assuming its peak tensile strength is normally about 10% of its compressive strength, the residual tensile stress of concrete can then be assumed to be 2% of its compressive strength.

### Determination of failure modes

By replacing some terms with their known quantities, the number of unknown variables in Eq. (10) is now reduced to three:  $\sigma_d$ ,  $f_v$ , and  $f_h$ . The variable  $\sigma_d$  is the compressive strength of cracked diagonal concrete struts ( $= -\zeta f'_c$ , with  $\zeta$  being the softening coefficient), and  $f_v$  and  $f_h$  are the stresses in the vertical and horizontal reinforcements at the time the wall fails, respectively. The maximum values of  $f_v$  and  $f_h$  are taken to be the smaller of 80% of yield strengths of the web reinforcements ( $0.8f_{yv}$  and  $0.8f_{yh}$ , respectively) and 500 MPa (72.52 ksi). The authors' experimental results on high-strength concrete (HSC) walls<sup>6</sup> show that most of the web reinforcements do not reach yield during testing. Thus, it is reasonable to take their maximum stresses to be 80% of their yield strengths. Moreover, it is also reasonable to assume that the maximum strengths are limited to 500 MPa (72.52 ksi) for typical shear reinforcement, as the use of higher strength reinforcement does not necessarily lead to stresses much higher than 500 MPa (72.52 ksi).

If the left-hand side of Eq. (10) is larger than the right-hand side, it means both web reinforcements reach their maximum strengths and the value of  $\sigma_d$  will be determined by the total value of the right-hand side. This also means that the  $\sigma_d$  is less than the compression capacity of the cracked diagonal concrete strut ( $-\zeta f'_c$ ). On the other hand, if the left-hand side of Eq. (10) is less than the right-hand side, it means the diagonal concrete strut fails in compression. In this case, the following assumption is made to calculate the stresses in web reinforcements. If the  $h_w/l_w$  is less than 1.0, it is assumed that only the vertical web reinforcement reaches its maximum strength, whereas if  $h_w/l_w$  is equal to or more than 1.0, it is assumed that only the horizontal web reinforcement reaches its maximum strength. These assumptions are based on data obtained from past experiment on RC walls<sup>19</sup> and the authors' own experimental study.<sup>6</sup> The remaining stress in the web reinforcement (either  $f_v$  or  $f_h$ ) can then be calculated.

### Softening coefficient of concrete struts

Numerous equations have been proposed to take into account the softening behavior of concrete under compression ( $\zeta$ ) when subjected to transverse strains.<sup>9,15,20,21</sup> A suit-

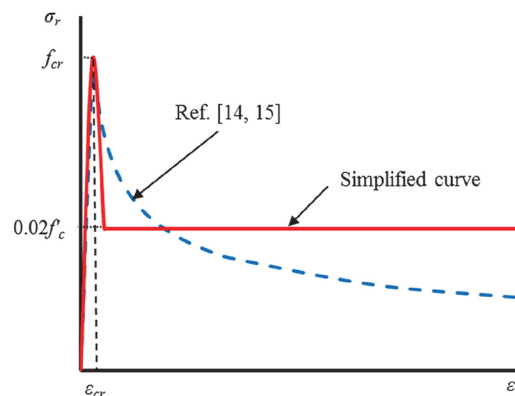


Fig. 3—Average stress-strain curve of concrete in tension.

able formula is introduced by Zhang and Hsu,<sup>21</sup> as shown in Eq. (11). In this proposed model, the value of  $\epsilon_r$  is approximated as 0.005, which falls within the typical range of  $\epsilon_r$  for RC membrane element subjected to shear<sup>9</sup>

$$\zeta = \left( \frac{5.8}{\sqrt{f'_c}} \leq 0.9 \right) \left( \frac{1}{\sqrt{1 + 400\epsilon_r}} \right) \quad (11)$$

where  $\zeta$  is the softening coefficient of the concrete in compression;  $f'_c$  is concrete cylinder compressive strength (in MPa); and  $\epsilon_r$  is principal strain of concrete in r-axis, positive for tension.

### Determination of angle of strut inclination

After all the terms in Eq. (10) are determined, the angle  $\theta$  of the diagonal concrete struts with respect to the horizontal axis can be calculated by rearranging Eq. (6) to become Eq. (12). Then, the nominal shear strength of RC wall ( $V_n$ ) can be calculated by multiplying the average shear stress ( $\tau_{vh}$ ) at the ultimate load stage, as defined in Eq. (8) by wall web area ( $A_w$ ). In this proposed model, the wall web area ( $A_w$ ) is defined as the thickness of wall web ( $t_w$ ) multiplied by the effective depth of wall ( $d_w$ ). The effective depth of wall can be taken as the distance between center to center of boundary elements, or  $0.8l_w$  (80% of wall length) in case of walls without boundary elements

$$\theta = \sin^{-1} \left( \sqrt{\frac{-\sigma_v + \sigma_r + \rho_v f_v}{-\sigma_d + \sigma_r}} \right) \quad (12)$$

where  $\theta$  is the angle of diagonal concrete strut (d-axis) with respect to horizontal axis at ultimate stage;  $\sigma_v$  is applied normal (vertical) stress, positive for tension;  $\sigma_d$  is principal stress of concrete in d-axis, positive for tension (normally compression);  $\sigma_r$  is principal stress of concrete in r-axis, positive for tension (normally tension);  $\rho_v$  is average vertical web reinforcement ratio; and  $f_v$  is average stress in the vertical web reinforcement.

### Dowel action from reinforced boundary elements

The inclusion of dowel action from reinforced boundary elements agrees with experimental findings<sup>22</sup> and is also

confirmed by the authors' experimental study.<sup>6</sup> The boundary elements can be in the form of flanges with reinforcement or columns at the ends of the wall with concentrated reinforcement. In this proposed model, the dowel action formula as developed by Baumann and Rusch<sup>23</sup> was adopted and shown in Eq. (13). This equation was also used by He<sup>24</sup> for predicting shear strengths of RC beams. In Eq. (13), the total area of the vertical reinforcement in one boundary element ( $A_{sb}$ ) is converted to a single dowel bar with the same area that has an equivalent bar diameter ( $d_{be}$ ). Then, the effective width of boundary element ( $b_{ef}$ ) can be calculated by subtracting the overall width of the boundary element ( $b_f$ ) with the equivalent bar diameter ( $d_{be}$ ). Here, the overall width of the boundary element ( $b_f$ ) does not need to be taken greater than half of wall height plus wall web thickness ( $0.5h_w + t_w$ ), as suggested by ACI 318 Chapter 18.<sup>4</sup> The dowel force  $D_u$  is then added as an additional component to the shear strength of RC walls.

Thus, the nominal shear strength of RC walls ( $V_n$ ) according to this proposed model can be expressed by Eq. (14). Note that in this proposed model, the dowel force is considered for one boundary element only (the one in tension) because the dowel force will become active following crack opening.

$$D_u = 1.64b_{ef}d_{be}\sqrt[3]{f'_c} \quad (13)$$

$$V_n = (\sigma_r - \sigma_d)\sin\theta\cos\theta t_w d_w + 1.64b_{ef}d_{be}\sqrt[3]{f'_c} \quad (14)$$

where  $D_u$  is dowel force of vertical reinforcement in one boundary element (in Newtons);  $b_{ef}$  is effective width of boundary element (in mm);  $d_{be}$  is equivalent bar diameter (in mm);  $V_n$  is nominal shear strength of RC wall (in Newtons);  $t_w$  is thickness of wall web (in mm); and  $d_w$  is effective depth of wall (in mm).

### Summary of new proposed method

Overall, the step-by-step procedure of the proposed method can be summarized as follows:

1. Calculate  $\sigma_r$  as  $0.02f'_c$  and  $\zeta$  using Eq. (11) assuming  $\epsilon_r$  is equal to 0.005.
2. Check if the web reinforcements reach their maximum strengths or if the diagonal concrete struts get crushed (use Eq. (10)).
  - a. If both web reinforcements reach their maximum strengths, then calculate the value of  $\sigma_d$ , which should be less than the compression capacity of cracked diagonal concrete struts ( $-\zeta f'_c$ ).
  - b. If the diagonal concrete struts crushed, then calculate the stresses in the shear reinforcements. For RC wall with  $h_w/l_w$  less than 1.0, assume  $f_v$  to be the smaller of  $0.8f_{yv}$  and 500 MPa (72.52 ksi), and then calculate  $f_h$ . Otherwise, assume  $f_h$  to be the smaller of  $0.8f_{yh}$  and 500 MPa (72.52 ksi), and then calculate  $f_v$ .
3. Calculate  $\theta$  using Eq. (12).
4. Calculate  $D_u$  using Eq. (13).
5. Calculate the ultimate or nominal shear strength  $V_n$  using Eq. (14).

### COMPARISON WITH EXPERIMENTAL RESULTS

To verify the accuracy of the proposed model, data from past experiments on RC walls failing in shear<sup>2,12,19,22,25-30</sup> as well as those from the experiment conducted by the authors<sup>6</sup> were used. The data are presented in Table 1. A total of 84 specimens were collected. The predictions of wall shear strengths using the proposed model were then compared with predictions from ACI 318, Eurocode 8, Hwang and Lee's method,<sup>11</sup> and Gupta and Rangan's method.<sup>12</sup> The ratios of the experimental shear strengths to calculated shear strengths ( $V_{exp}/V_n$ ) were plotted against height-to-length ratios of walls ( $h_w/l_w$ ), concrete compressive strength ( $f'_c$ ), and vertical reinforcement ratio in the boundary element ( $\rho_b$ ) in order to see the variation of predictions as influenced by these parameters. The analysis results are presented in Table 2 and Fig. 4, 5, and 6. In Fig. 4, 5, and 6, only  $V_{exp}/V_n$  values from ACI 318 and the authors' proposed model are plotted while the other methods are represented by their trend lines that show the average values of  $V_{exp}/V_n$  within certain ranges of the parameters.

From the experimental comparisons (Table 2), it can be seen that the authors' proposed model is more accurate than the other four methods. This is shown by the average value of  $V_{exp}/V_n$  of 1.36, with the lowest coefficient of variation (COV) of 0.20. It should be noted, however, that the predictions of the authors' proposed model are mostly quite conservative ( $V_{exp}/V_n$  greater than 2.00) for shorter walls with  $h_w/l_w$  less than 0.5, as tested by Barda et al.<sup>19</sup> On the other hand, for taller walls with  $h_w/l_w$  greater than 2.0, as tested by Corley et al.,<sup>22</sup> the predictions of the authors' proposed model are not conservative enough for some cases ( $V_{exp}/V_n$  less than 1.00). As can be seen in Table 2 that Hwang-Lee's model<sup>11</sup> is reasonably accurate ( $V_{exp}/V_n = 1.29$  and COV = 0.33), but it overestimates the shear strengths of many walls, whereas the authors' proposed model only overestimates six walls out of 84 specimens. Eurocode 8<sup>5</sup> is the most conservative one, with an average value of  $V_{exp}/V_n$  of 2.13 and minimum value of 1.21 with COV of 0.35. Gupta-Rangan's model<sup>12</sup> has the highest COV (0.75) while their average value of  $V_{exp}/V_n$  is 1.59.

From Fig. 4 to 6, it can be seen that the predictions of the authors' proposed model are uniformly accurate (average values are quite consistent) for  $V_{exp}/V_n$  versus various ranges of parameters, and they are less scattered compared to predictions by other methods. From Fig. 4, it can be seen that for walls with  $h_w/l_w$  greater than 2.0, the predictions of the authors' proposed model are less conservative, whereas Gupta-Rangan's model<sup>12</sup> predictions are overly conservative. From Fig. 5, it can be seen that as the concrete compressive strength increases, predictions by other methods become less accurate whereas the authors' proposed model are quite consistent, even for HSC walls. From Fig. 6, it can be seen that as the ratio of vertical reinforcement in boundary element increases, the predictions by other methods become less accurate whereas the authors' proposed model predictions are quite consistent because the model takes into account the dowel action from the reinforced boundary elements. This clearly shows that inclusion of dowel action is quite important to predict more accurately RC wall shear strengths.

**Table 1—Experimental data of RC walls failing in shear**

No.	Specimen ID	$f'_c$ , MPa	$A_g$ , mm <sup>2</sup>	$P_s$ , kN	$h_w$ , mm	$l_w$ , mm	$t_w$ , mm	$b_f$ , mm	$t_f$ , mm	$\rho_b$	$f_{yb}$ , MPa	$\rho_v$	$f_{yv}$ , MPa	$\rho_h$	$f_{yh}$ , MPa	$V_{exp}$ , kN	Loading type
Barda et al. <sup>19</sup>																	
1	B1-1	29	296,774	0	876	1905	102	610	102	0.0180	525	0.0050	543	0.0050	496	1218	M
2	B2-1	16	296,774	0	876	1905	102	610	102	0.0640	487	0.0050	552	0.0050	499	978	M
3	B3-2	27	296,774	0	876	1905	102	610	102	0.0410	414	0.0050	545	0.0050	513	1108	C
4	B6-4	21	296,774	0	876	1905	102	610	102	0.0410	529	0.0025	496	0.0050	496	876	C
5	B7-5	26	296,774	0	400	1905	102	610	102	0.0410	539	0.0050	531	0.0050	501	1140	C
6	B8-5	23	296,774	0	1829	1905	102	610	102	0.0410	489	0.0050	527	0.0050	496	886	C
Cardenas et al. <sup>2</sup>																	
7	SW-7	43	145,161	0	1905	1905	76	76	191	0.0767	448	0.0077	448	0.0027	414	519	M
8	SW-8	42	145,161	0	1905	1905	76	76	191	0.0300	448	0.0300	448	0.0027	465	570	M
Corley et al. <sup>22</sup>																	
9	B2	54	317,419	49	4572	1905	102	305	305	0.0367	410	0.0029	532	0.0063	532	680	C
10	B5	45	317,419	49	4572	1905	102	305	305	0.0367	444	0.0029	502	0.0063	502	762	C
11	B6	22	317,419	979	4572	1905	102	305	305	0.0367	441	0.0029	512	0.0063	512	825	C
12	B7	49	317,419	1241	4572	1905	102	305	305	0.0367	458	0.0029	490	0.0063	490	980	C
13	B8	42	317,419	1241	4572	1905	102	305	305	0.0367	447	0.0029	454	0.0138	482	978	C
14	B9	44	317,419	1241	4572	1905	102	305	305	0.0367	430	0.0029	461	0.0063	461	977	C
15	B10	46	317,419	1241	4572	1905	102	305	305	0.0197	443	0.0029	464	0.0063	464	707	C
16	F1	38	358,709	49	4572	1905	102	914	102	0.0389	445	0.0030	525	0.0071	525	836	C
17	F2	46	358,709	1241	4572	1905	102	914	102	0.0435	430	0.0031	464	0.0063	464	887	C
Maeda <sup>25</sup>																	
18	MAE03	58	210,400	412	1200	2180	80	180	180	0.0781	389	0.0119	321	0.0119	321	1460	C
19	MAE07	58	210,400	412	1200	2180	80	180	180	0.0781	389	0.0200	321	0.0200	321	1676	C
Okamoto <sup>26</sup>																	
20	W48M6	82	369,600	725	1280	1720	120	800	120	0.0089	560	0.0079	560	0.0079	560	1516	C
21	W48M4	82	369,600	725	1280	1720	120	800	120	0.0119	347	0.0119	347	0.0119	347	1479	C
22	W72M8	82	369,600	725	1280	1720	120	800	120	0.0089	792	0.0091	792	0.0091	792	2066	C
23	W72M6	82	369,600	725	1280	1720	120	800	120	0.0119	560	0.0119	560	0.0119	560	2015	C
24	W72M8	102	369,600	725	1280	1720	120	800	120	0.0089	792	0.0091	792	0.0091	792	2128	C
25	W96M8	102	369,600	725	1280	1720	120	800	120	0.0119	792	0.0119	792	0.0119	792	2483	C
Mo and Chan <sup>27</sup>																	
26	HN4-1	32	76,200	0	500	860	70	170	80	0.0210	302	0.0073	302	0.0081	302	205	C
27	HN4-2	32	76,200	0	500	860	70	170	80	0.0210	302	0.0073	302	0.0081	302	247	C
28	HN4-3	32	76,200	0	500	860	70	170	80	0.0210	302	0.0073	302	0.0081	302	202	C
29	HN6-1	30	76,200	0	500	860	70	170	80	0.0210	443	0.0073	443	0.0081	443	255	C
30	HN6-2	30	76,200	0	500	860	70	170	80	0.0210	443	0.0073	443	0.0081	443	204	C
31	HN6-3	31	76,200	0	500	860	70	170	80	0.0210	443	0.0073	443	0.0081	443	205	C
32	HM4-1	38	76,200	0	500	860	70	170	80	0.0210	302	0.0073	302	0.0081	302	223	C
33	HM4-2	38	76,200	0	500	860	70	170	80	0.0210	302	0.0073	302	0.0081	302	231	C
34	HM4-3	40	76,200	0	500	860	70	170	80	0.0210	302	0.0073	302	0.0081	302	250	C
35	LN4-1	18	76,200	0	500	860	70	170	80	0.0210	302	0.0058	302	0.0081	302	193	C
36	LN4-2	18	76,200	0	500	860	70	170	80	0.0210	302	0.0058	302	0.0081	302	217	C
37	LN4-3	30	76,200	0	500	860	70	170	80	0.0210	302	0.0058	302	0.0081	302	203	C
38	LN6-1	31	76,200	0	500	860	70	170	80	0.0210	443	0.0058	443	0.0081	443	246	C
39	LN6-2	30	76,200	0	500	860	70	170	80	0.0210	443	0.0058	443	0.0081	443	200	C
40	LN6-3	30	76,200	0	500	860	70	170	80	0.0210	443	0.0058	443	0.0081	443	210	C
41	LM6-1	39	76,200	0	500	860	70	170	80	0.0210	443	0.0058	443	0.0081	443	219	C

**Table 1 (cont.)—Experimental data of RC walls failing in shear**

42	LM6-2	37	76,200	0	500	860	70	170	80	0.0210	443	0.0058	443	0.0081	443	205	C
43	LM6-3	35	76,200	0	500	860	70	170	80	0.0210	443	0.0058	443	0.0081	443	210	C
44	LM4-2	66	76,200	0	500	860	70	170	80	0.0210	302	0.0058	302	0.0081	302	250	C
45	LM4-3	66	76,200	0	500	860	70	170	80	0.0210	302	0.0058	302	0.0081	302	227	C
Gupta and Rangan <sup>12</sup>																	
46	S-1	79	135,000	0	1000	1000	75	375	100	0.0210	535	0.0100	545	0.0050	578	428	M
47	S-2	65	135,000	610	1000	1000	75	375	100	0.0304	535	0.0100	545	0.0050	578	720	M
48	S-3	69	135,000	1230	1000	1000	75	375	100	0.0387	535	0.0100	545	0.0050	578	851	M
49	S-4	75	135,000	0	1000	1000	75	375	100	0.0315	535	0.0150	533	0.0050	578	600	M
50	S-5	73	135,000	610	1000	1000	75	375	100	0.0399	535	0.0150	533	0.0050	578	790	M
51	S-6	71	135,000	1230	1000	1000	75	375	100	0.0446	535	0.0150	533	0.0050	578	970	M
52	S-7	71	135,000	610	1000	1000	75	375	100	0.0304	535	0.0100	545	0.0100	545	800	M
Kabeyasawa and Hiraishi <sup>28</sup>																	
53	W-08	103	184,000	1764	2000	1700	80	200	200	0.0214	761	0.0053	1079	0.0053	1079	1670	C
54	W-12	138	184,000	2313	2000	1700	80	200	200	0.0214	761	0.0053	1079	0.0053	1079	1719	C
55	No. 1	65	184,000	1568	2000	1700	80	200	200	0.0508	1009	0.0020	792	0.0020	792	1101	C
56	No. 2	71	184,000	1568	2000	1700	80	200	200	0.0508	1009	0.0035	792	0.0035	792	1255	C
57	No. 3	72	184,000	1568	2000	1700	80	200	200	0.0508	1009	0.0053	792	0.0053	792	1379	C
58	No. 4	103	184,000	2617	2000	1700	80	200	200	0.0508	1009	0.0053	792	0.0053	792	1697	C
59	No. 5	77	184,000	1568	3000	1700	80	200	200	0.0508	1009	0.0053	792	0.0053	792	1159	C
60	No. 6	74	184,000	1568	2000	1700	80	200	200	0.0508	1009	0.0066	1420	0.0066	1420	1412	C
61	No. 7	72	184,000	1568	2000	1700	80	200	200	0.0508	1009	0.0100	792	0.0100	792	1499	C
62	No. 8	76	184,000	1568	2000	1700	80	200	200	0.0508	1009	0.0145	792	0.0145	792	1639	C
Farvashany et al. <sup>29</sup>																	
63	HSCW1	104	120,000	540	1100	880	75	375	90	0.0400	670	0.0126	535	0.0047	535	735	M
64	HSCW2	93	120,000	954	1100	880	75	375	90	0.0400	670	0.0126	535	0.0047	535	845	M
65	HSCW3	86	120,000	953	1100	880	75	375	90	0.0400	670	0.0075	535	0.0047	535	625	M
66	HSCW4	91	120,000	2364	1100	880	75	375	90	0.0400	670	0.0075	535	0.0047	535	866	M
67	HSCW5	84	120,000	955	1100	880	75	375	90	0.0400	670	0.0126	535	0.0075	535	801	M
68	HSCW6	90	120,000	550	1100	880	75	375	90	0.0400	670	0.0126	535	0.0075	535	745	M
69	HSCW7	102	120,000	952	1100	880	75	375	90	0.0400	670	0.0075	535	0.0075	535	800	M
Burgueno et al. <sup>30</sup>																	
70	M05C	46	167,640	579	2286	1016	76	254	254	0.0556	491	0.0147	445	0.0183	445	803	C
71	M05M	39	167,640	579	2286	1016	76	254	254	0.0556	491	0.0147	445	0.0183	445	855	M
72	M10C	56	167,640	579	2286	1016	76	254	254	0.0556	457	0.0147	476	0.0183	476	751	C
73	M10M	84	167,640	579	2286	1016	76	254	254	0.0556	457	0.0147	476	0.0183	476	900	M
74	M15C	102	167,640	579	2286	1016	76	254	254	0.0528	439	0.0147	481	0.0183	481	819	C
75	M15M	111	167,640	579	2286	1016	76	254	254	0.0556	514	0.0147	478	0.0183	478	934	M
76	M20C	131	167,640	579	2286	1016	76	254	254	0.0556	449	0.0147	438	0.0244	438	815	C
77	M20M	115	167,640	579	2286	1016	76	254	254	0.0556	449	0.0147	438	0.0244	438	923	M
Teng and Chandra <sup>6</sup>																	
78	J1	103	196,000	1012	1000	1000	100	500	120	0.0388	630	0.0028	610	0.0028	610	1210	C
79	J2	97	196,000	949	1000	1000	100	500	120	0.0388	630	0.0075	578	0.0028	610	1271	C
80	J3	111	196,000	1085	1000	1000	100	500	120	0.0388	630	0.0028	610	0.0075	578	1459	C
81	J4	94	111,200	520	1000	1000	100	120	280	0.0693	630	0.0028	610	0.0028	610	811	C
82	J5	103	196,000	1012	2000	1000	100	500	120	0.0388	630	0.0028	610	0.0028	610	596	C
83	J6	97	196,000	949	2000	1000	100	500	120	0.0388	630	0.0075	578	0.0028	610	724	C
84	J7	111	196,000	1085	2000	1000	100	500	120	0.0388	630	0.0028	610	0.0075	578	895	C

Notes: 1 MPa = 145 psi; 1 mm = 0.0394 in.; 1 kN = 0.225 kip. Loading type: M is monotonic; and C is cyclic.



**Table 2—Experimental and calculated wall shear strengths**

No.	Specimen ID	$f'_c$ , MPa	$h_w/l_w$	$V_{exp}/V_n$				
				ACI 318	Eurocode 8	Hwang-Lee <sup>11</sup>	Gupta and Rangan <sup>12</sup>	Proposed model
Barda et al. <sup>19</sup>								
1	B1-1	29	0.46	1.65	3.94	1.23	0.98	2.11
2	B2-1	16	0.46	1.51	3.45	1.72	1.17	1.70
3	B3-2	27	0.46	1.48	3.23	1.18	0.91	1.80
4	B6-4	21	0.46	1.25	2.72	1.39	1.50	1.92
5	B7-5	26	0.21	1.56	4.64	1.09	1.16	2.18
6	B8-5	23	0.96	1.24	2.24	1.82	1.66	1.46
Cardenas et al. <sup>2</sup>								
7	SW-7	43	1.00	1.30	2.06	0.88	1.11	1.54
8	SW-8	42	1.00	1.36	2.02	0.97	0.37	0.93
Corley et al. <sup>22</sup>								
9	B2	54	2.40	0.76	1.31	1.04	5.73	1.15
10	B5	45	2.40	0.91	1.56	1.27	6.77	1.41
11	B6	22	2.40	1.10	1.96	1.56	2.58	1.21
12	B7	49	2.40	1.18	2.05	1.11	2.65	1.17
13	B8	42	2.40	0.94	1.38	1.13	2.69	0.92
14	B9	44	2.40	1.25	2.17	1.12	2.68	1.23
15	B10	46	2.40	0.90	1.56	0.81	1.94	0.90
16	F1	38	2.40	0.90	1.45	1.41	6.19	0.99
17	F2	46	2.40	1.13	1.96	0.91	2.31	0.79
Maeda <sup>25</sup>								
18	MAE03	58	0.55	1.46	2.82	1.02	0.81	1.69
19	MAE07	58	0.55	1.52	2.38	1.10	0.68	1.40
Okamoto <sup>26</sup>								
20	W48M6	82	0.74	1.10	1.99	0.88	0.88	1.13
21	W48M4	82	0.74	1.12	1.97	0.86	0.90	1.13
22	W72M8	82	0.74	1.33	1.89	1.20	0.83	1.35
23	W72M6	82	0.74	1.30	1.93	1.17	0.86	1.18
24	W72M8	102	0.74	1.23	1.93	1.14	0.86	1.31
25	W96M8	102	0.74	1.44	2.04	1.33	0.81	1.30
Mo and Chan <sup>27</sup>								
26	HN4-1	32	0.58	0.88	1.58	0.87	0.91	1.35
27	HN4-2	32	0.58	1.06	1.90	1.05	1.10	1.63
28	HN4-3	32	0.58	0.87	1.56	0.86	0.90	1.33
29	HN6-1	30	0.58	0.94	1.70	1.18	0.77	1.30
30	HN6-2	30	0.58	0.75	1.36	0.95	0.62	1.04
31	HN6-3	31	0.58	0.74	1.31	0.90	0.62	1.04
32	HM4-1	38	0.58	0.93	1.69	0.81	1.00	1.41
33	HM4-2	38	0.58	0.96	1.75	0.84	1.04	1.46
34	HM4-3	40	0.58	1.03	1.88	0.86	1.12	1.55
35	LN4-1	18	0.58	0.91	2.00	1.47	1.04	1.57
36	LN4-2	18	0.58	1.02	2.25	1.65	1.17	1.76
37	LN4-3	30	0.58	0.88	1.59	0.93	1.12	1.47
38	LN6-1	31	0.58	0.89	1.58	1.10	0.93	1.35
39	LN6-2	30	0.58	0.73	1.30	0.91	0.76	1.10
40	LN6-3	30	0.58	0.76	1.37	0.95	0.80	1.16
41	LM6-1	39	0.58	0.70	1.28	0.76	0.84	1.14
42	LM6-2	37	0.58	0.67	1.21	0.76	0.78	1.08
43	LM6-3	35	0.58	0.72	1.24	0.83	0.80	1.12
44	LM4-2	66	0.58	0.92	1.78	0.69	1.40	1.37

**Table 2 (cont.)—Experimental and calculated wall shear strengths**

45	LM4-3	66	0.58	0.84	1.62	0.63	1.27	1.24
Gupta and Rangan <sup>12</sup>								
46	S-1	79	1.00	1.11	1.58	0.99	1.12	1.07
47	S-2	65	1.00	1.96	2.24	1.32	1.03	1.46
48	S-3	69	1.00	2.28	2.28	1.23	0.88	1.43
49	S-4	75	1.00	1.58	2.16	1.43	1.07	1.30
50	S-5	73	1.00	2.10	2.43	1.42	0.90	1.41
51	S-6	71	1.00	2.59	2.60	1.40	0.94	1.52
52	S-7	71	1.00	1.52	2.05	1.41	1.15	1.32
Kabeyasawa and Hiraishi <sup>28</sup>								
53	W-08	103	1.18	1.48	1.93	1.35	1.10	1.62
54	W-12	138	1.18	1.46	1.95	1.21	0.95	1.40
55	No. 1	65	1.18	2.25	2.19	1.11	1.04	1.70
56	No. 2	71	1.18	1.90	1.93	1.18	1.06	1.61
57	No. 3	72	1.18	1.60	1.84	1.23	1.03	1.51
58	No. 4	103	1.18	1.84	1.88	1.22	0.94	1.42
59	No. 5	77	1.76	1.41	1.50	1.07	1.31	1.25
60	No. 6	74	1.18	1.45	1.86	1.26	1.01	1.40
61	No. 7	72	1.18	1.57	2.01	1.34	1.00	1.22
62	No. 8	76	1.18	1.66	2.13	1.45	1.01	1.07
Farvashany et al. <sup>29</sup>								
63	HSCW1	104	1.25	2.20	2.36	1.56	1.34	1.41
64	HSCW2	93	1.25	2.60	2.48	1.60	1.18	1.52
65	HSCW3	86	1.25	1.96	1.85	1.19	1.07	1.22
66	HSCW4	91	1.25	2.68	1.99	1.13	0.84	1.28
67	HSCW5	84	1.25	1.93	2.07	1.42	1.12	1.32
68	HSCW6	90	1.25	1.77	1.94	1.49	1.35	1.34
69	HSCW7	102	1.25	1.85	1.94	1.39	1.37	1.34
Burgueno et al. <sup>30</sup>								
70	M05C	46	2.25	1.85	2.68	2.46	3.05	1.43
71	M05M	39	2.25	2.14	3.23	2.76	3.46	1.55
72	M10C	56	2.25	1.56	2.19	2.22	2.73	1.24
73	M10M	84	2.25	1.53	2.09	2.43	3.27	1.39
74	M15C	102	2.25	1.27	1.77	2.09	2.96	1.21
75	M15M	111	2.25	1.38	1.98	2.33	3.39	1.35
76	M20C	131	2.25	1.11	1.72	1.92	3.13	1.08
77	M20M	115	2.25	1.34	1.95	2.27	3.55	1.26
Teng and Chandra <sup>6</sup>								
78	J1	103	1.00	2.85	3.25	1.62	1.93	1.82
79	J2	97	1.00	3.05	3.48	1.75	1.52	1.83
80	J3	111	1.00	2.09	2.36	1.71	2.21	1.77
81	J4	94	1.00	1.97	2.35	1.44	1.71	2.07
82	J5	103	2.00	1.73	4.36	1.07	1.92	0.90
83	J6	97	2.00	2.14	5.30	1.33	1.75	1.04
84	J7	111	2.00	1.46	2.58	1.23	2.74	1.09
Statistical parameters								
Minimum value				0.67	1.21	0.63	0.37	0.79
Maximum value				3.05	5.30	2.76	6.77	2.18
Average value				1.43	2.13	1.29	1.59	1.36
Standard deviation				0.54	0.74	0.43	1.19	0.28
Coefficient of variation				0.38	0.35	0.33	0.75	0.20

Note: 1 MPa = 145 psi.

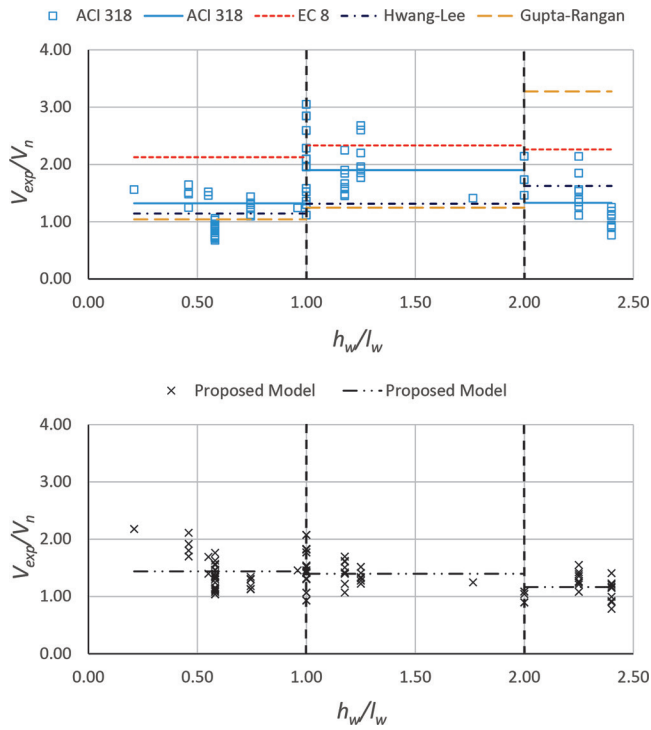


Fig. 4— $V_{exp}/V_n$  plotted against height-to-length ratio ( $h_w/l_w$ ).

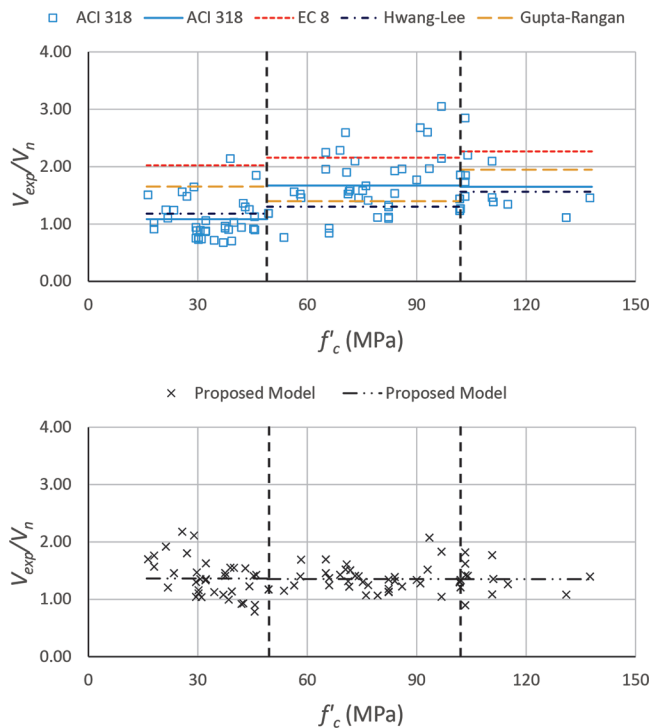


Fig. 5— $V_{exp}/V_n$  plotted against concrete compressive strength ( $f'_c$ ).

## CONCLUSIONS

The authors have presented an analytical model based on the principles of truss analogy to calculate the shear strengths of high-strength as well as normal-strength concrete walls. The following conclusions can be made:

1. The effective contributions of the vertical and horizontal shear reinforcements to the overall shear strengths of walls are dependent on wall height-to-length ratio ( $h_w/l_w$ ). As the  $h_w/l_w$

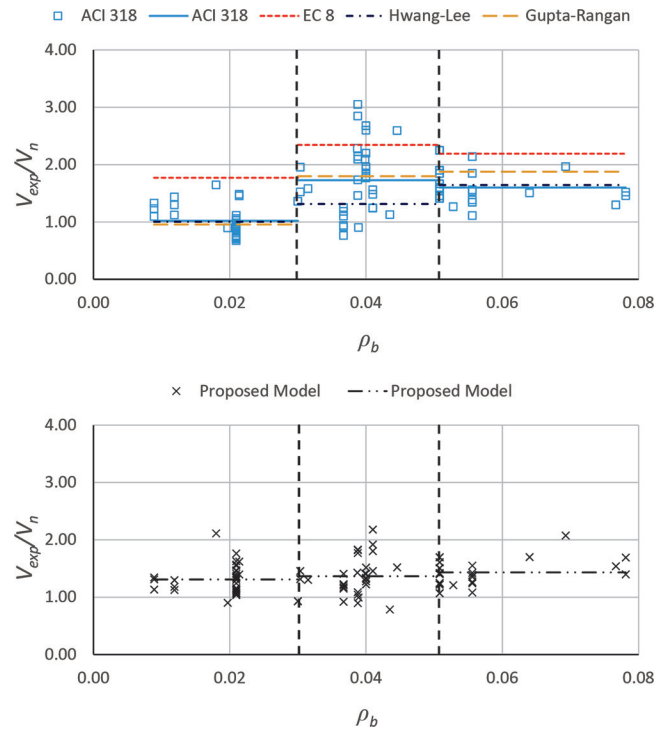


Fig. 6— $V_{exp}/V_n$  plotted against ratio of vertical reinforcement in boundary element ( $\rho_b$ ). Note:  $\rho_b = A_{sb}/(b_f \times t_f)$ .

becomes higher than 1.0, the horizontal web reinforcement becomes more effective than the vertical web reinforcement. This is represented correctly in the authors' model.

2. The contribution of dowel action from the reinforced boundary elements is significant and it has been confirmed by various researchers<sup>22</sup> as well as by the authors.<sup>6</sup> The presence of boundary elements or flanges increases the shear strength significantly beyond the additional area of the flanges.

3. The proposed model was verified with a total of 84 RC wall specimens failing in shear that were selected from available literature<sup>2,12,19,22,25-30</sup> as well as from the authors' own experimental study,<sup>6</sup> and it is confirmed to be reasonably accurate.

4. Compared to the methods by Hwang and Lee<sup>11</sup> and Gupta and Rangan,<sup>12</sup> as well as the methods in the ACI 318 and Eurocode 8, the predictions of the authors' proposed model are more accurate in the sense that it has the average value of  $V_{exp}/V_n$  of 1.36 with the lowest COV of 0.20. The proposed method is also able to predict the shear strength of RC walls with consistent accuracy for wide ranges of wall height-to-length ratios, concrete compressive strengths, and percentage of reinforcements in the boundary elements.

## AUTHOR BIOS

**Jimmy Chandra** is a Lecturer at Petra Christian University, Indonesia. He received his bachelor of engineering degree from Petra Christian University, his master of engineering degree from Asian Institute of Technology, Thailand, and his doctor of philosophy degree from Nanyang Technological University, Singapore. His research interests include behavior and seismic performance evaluation of reinforced concrete structures.

**Khatthanam Chanthabouala** is a Civil and Structural Engineer. He received his bachelor of engineering degree and his doctor of philosophy degree from Nanyang Technological University. His research interests include behavior of high-strength concrete and steel fiber-reinforced concrete flat plate structures.

ACI member **Susanto Teng** is an Associate Professor at Nanyang Technological University, Singapore. He is a member of ACI Committee 435, Deflection of Concrete Building Structures; and Joint ACI-ASCE Committees 421, Design of Reinforced Concrete Slabs, and 445, Shear and Torsion. His research interests include behavior of structural concrete walls, shear strength of slabs, size effect in shear behavior of concrete members, computational modeling of concrete structures, and durability of marine concrete structures.

## ACKNOWLEDGMENTS

This research is part of the Competitive Research Program “Underwater Infrastructure and Underwater City of the Future” funded by the National Research Foundation (NRF) of Singapore. The authors are grateful for the funding. Support by Nanyang Technological University, Singapore, through the School of Civil and Environmental Engineering is also very much appreciated.

## NOTATION

$A_{cv}$  = gross area of concrete section bounded by web thickness and length of section in the direction of shear force considered  
 $A_{cw}$  = area of concrete section of individual vertical wall segment considered  
 $A_g$  = wall gross cross-section area  
 $A_{sb}$  = total area of vertical reinforcement in one boundary element  
 $A_{str}$  = area of diagonal concrete strut  
 $A_{sw}$  = cross-sectional area of shear reinforcement  
 $A_w$  = wall web area  
 $b_{ef}$  = effective width of boundary element  
 $b_f$  = width of boundary element  
 $b_w$  = minimum width (thickness) of wall between tension and compression chords  
 $b_{wo}$  = width of wall web  
 $C_d$  = diagonal compression force acting on nodal zone  
 $C_{d,n}$  = nominal capacity of nodal zone  
 $D$  = compression force in diagonal strut  
 $D_u$  = dowel force of vertical reinforcement in one boundary element  
 $d_{pe}$  = equivalent bar diameter  
 $d_w$  = effective depth of wall  
 $F_h$  = tension force in the horizontal tie.  
 $F_v$  = tension force in the vertical tie  
 $f_c'$  = concrete cylinder compressive strength  
 $f_{cd}$  = design value of concrete compressive strength  
 $f_{ck}$  = characteristic compressive cylinder strength of concrete at 28 days  
 $f_{cr}$  = cracking stress of concrete  
 $f_h$  = average stress in horizontal web reinforcement  
 $f_v$  = average stress in the vertical web reinforcement  
 $f_y$  = specified yield strength of reinforcement  
 $f_{yb}$  = yield strength of vertical reinforcement in boundary element  
 $f_{y,h}$  = design value of yield strength of horizontal web reinforcement  
 $f_{y,h}$  = yield strength of horizontal shear reinforcement  
 $f_{y,v}$  = yield strength of vertical shear reinforcement  
 $f_{y,wd}$  = design yield strength of shear reinforcement  
 $h_w$  = height of wall  
 $K$  = strut-and-tie index  
 $l_w$  = wall length  
 $M_{Ed}$  = design bending moment at base of wall  
 $P$  = axial load applied at top of wall  
 $s$  = spacing of horizontal shear (web) reinforcement  
 $t_f$  = thickness of boundary element  
 $t_w$  = thickness of wall web  
 $V$  = applied external shear force  
 $V_{Ed}$  = design shear force  
 $V_{exp}$  = experimental wall shear strength  
 $V_n$  = nominal shear strength of RC wall  
 $V_{Rd}$  = shear resistance of a member with shear reinforcement  
 $V_{Rd,c}$  = design shear resistance of a member without shear reinforcement  
 $V_{Rd,max}$  = design value of maximum shear force that can be sustained by the member  
 $V_{Rd,s}$  = design value of shear force that can be sustained by yielding shear reinforcement  
 $z$  = inner lever arm, which is taken as  $0.8l_w$  ( $l_w$  is wall length)  
 $\alpha$  = average strut angle with respect to longitudinal (vertical) axis  
 $\alpha_c$  = coefficient defining the relative contribution of concrete strength to nominal wall shear strength, which may be taken as 0.25 for  $h_w/l_w \leq 1.5$ , 0.17 for  $h_w/l_w \geq 2.0$ , and varies linearly between 0.25

and 0.17 for  $h_w/l_w$  between 1.5 and 2.0;  $h_w/l_w$  is the height-to-length ratio of the wall  
 $\alpha_{cw}$  = coefficient taking account of the state of the stress in the compression chord  
 $\epsilon_{cr}$  = cracking strain of concrete  
 $\epsilon_r$  = principal strain of concrete in r-axis, positive for tension  
 $\epsilon_t$  = average strain of wall panel in transverse direction, positive for tension  
 $\zeta$  = softening coefficient of concrete in compression  
 $\lambda$  = modification factor reflecting reduced mechanical properties of lightweight concrete, all relative to normalweight concrete of the same compressive strength  
 $\theta$  = angle between concrete compression strut and wall axis perpendicular to shear force (Eurocode 8)  
 $\theta$  = angle of inclination of diagonal compression strut with respect to horizontal axis (Hwang and Lee’s method)  
 $\theta$  = angle of diagonal concrete strut (d-axis) with respect to horizontal axis at ultimate stage (new proposed method)  
 $\nu_1$  = strength reduction factor for concrete cracked in shear  
 $\rho_b$  = ratio of vertical reinforcement in boundary element  
 $\rho_h$  = average horizontal web reinforcement ratio  
 $\rho_t$  = ratio of area of distributed transverse (horizontal) shear reinforcement to gross concrete area perpendicular to that reinforcement  
 $\rho_v$  = average vertical web reinforcement ratio  
 $\sigma_{cp}$  = mean compressive stress, measured positive, in concrete due to design axial force  
 $\sigma_d$  = principal stress of concrete in d-axis, positive for tension  
 $\sigma_h$  = applied normal stress in horizontal axis, positive for tension  
 $\sigma_r$  = principal stress of concrete in r-axis, positive for tension  
 $\sigma_t$  = normal stress in transverse direction, positive for tension  
 $\sigma_v$  = applied normal stress in vertical axis, positive for tension  
 $\tau_{vh}$  = average shear stress in v-h coordinate system and is due to shear force acting on the wall

## REFERENCES

- Cardenas, A. E., and Magura, D. D., “Strength of High-Rise Shear Walls—Rectangular Cross Section,” *Response of Multistory Concrete Structures to Lateral Forces*, SP-36, M. Fintel and J. G. MacGregor, eds., American Concrete Institute, Farmington Hills, MI, 1972, pp. 119-150.
- Cardenas, A. E.; Russell, H. G.; and Corley, W. G., “Strength of Low-Rise Structural Walls,” *Reinforced Concrete Structures Subjected to Wind and Earthquake Loads*, SP-63, J. Schwaighofer, ed., American Concrete Institute, Farmington Hills, MI, 1980, pp. 221-242.
- Park, R., and Paulay, T., *Reinforced Concrete Structures*, John Wiley & Sons, Inc., New York, 1975, 769 pp.
- ACI Committee 318, “Building Code Requirements for Structural Concrete (ACI 318-14) and Commentary (ACI 318R-14),” American Concrete Institute, Farmington Hills, MI, 2014, 520 pp.
- Comite Europeen de Normalisation, “Eurocode 8: Design of Structures for Earthquake Resistance Part 1: General Rules, Seismic Actions and Rules for Buildings (EN 1998-1),” Comite Europeen de Normalisation (CEN), Brussels, 2004.
- Teng, S., and Chandra, J., “Cyclic Shear Behavior of High Strength Concrete Structural Walls,” *ACI Structural Journal*, V. 113, No. 6, Nov.-Dec. 2016, pp. 1335-1345. doi: 10.14359/51689158
- Bazant, Z. P., “Microplane Model for Strain Controlled Inelastic Behavior,” *Mechanics of Engineering Materials*, Wiley, London, UK, Chapter 3, 1984, p. 45-59.
- Okamura, H., and Maekawa, K., “Nonlinear Analysis and Constitutive Models of Reinforced Concrete,” University of Tokyo, Tokyo, Japan, 1991, 182 pp.
- Vecchio, F. J., and Collins, M. P., “Modified Compression-Field Theory for Reinforced Concrete Elements Subjected to Shear,” *ACI Journal Proceedings*, V. 83, No. 2, Mar.-Apr. 1986, pp. 219-231.
- Hsu, T. T. C., “Softened Truss Model Theory for Shear and Torsion,” *ACI Structural Journal*, V. 85, No. 6, Nov.-Dec. 1988, pp. 624-635.
- Hwang, S. J., and Lee, H. J., “Strength Prediction for Discontinuity Regions by Softened Strut-and-Tie Model,” *Journal of Structural Engineering*, ASCE, V. 128, No. 12, 2002, pp. 1519-1526. doi: 10.1061/(ASCE)0733-9445(2002)128:12(1519)
- Gupta, A., and Rangan, B. V., “High-Strength Concrete (HSC) Structural Walls,” *ACI Structural Journal*, V. 95, No. 2, Mar.-Apr. 1998, pp. 194-204.
- Collins, M. P.; Mitchell, D.; and MacGregor, J. G., “Structural Design Considerations for High-Strength Concrete,” *Concrete International*, V. 15, No. 5, May 1993, pp. 27-34.

14. Belarbi, A., and Hsu, T. T. C., "Constitutive Laws of Concrete in Tension and Reinforcing Bars Stiffened by Concrete," *ACI Structural Journal*, V. 91, No. 4, July-Aug. 1994, pp. 465-474.
15. Pang, X. B., and Hsu, T. T. C., "Behavior of Reinforced Concrete Membrane Elements in Shear," *ACI Structural Journal*, V. 92, No. 6, Nov.-Dec. 1995, pp. 665-679.
16. Reinhardt, H. W.; Cornelissen, H. A. W.; and Hordijk, D. A., "Tensile Tests and Failure Analysis of Concrete," *Journal of Structural Engineering*, ASCE, V. 112, No. 11, 1986, pp. 2462-2477. doi: 10.1061/(ASCE)0733-9445(1986)112:11(2462)
17. Yankelevsky, D. Z., and Reinhardt, H. W., "Uniaxial Behavior of Concrete in Cyclic Tension," *Journal of Structural Engineering*, ASCE, V. 115, No. 1, 1989, pp. 166-182. doi: 10.1061/(ASCE)0733-9445(1989)115:1(166)
18. Laskar, A.; Wang, J.; Hsu, T. T. C.; and Mo, Y. L., "Rational Shear Provisions for AASHTO LRFD Specifications: Technical Report," University of Houston, Houston, TX, 2007, 216 pp.
19. Barda, F.; Hanson, J. M.; and Corley, W. G., "Shear Strength of Low-Rise Walls with Boundary Elements," Reinforced Concrete Structures in Seismic Zones, SP-53, N. M. Hawkins and D. Mitchell, eds., American Concrete Institute, Farmington Hills, MI, 1977, pp. 149-202.
20. Belarbi, A., and Hsu, T. T. C., "Constitutive Laws of Softened Concrete in Biaxial Tension-Compression," *ACI Structural Journal*, V. 92, No. 5, Sept.-Oct. 1995, pp. 562-573.
21. Zhang, L. X., and Hsu, T. T. C., "Behavior and Analysis of 100 MPa Concrete Membrane Elements," *Journal of Structural Engineering*, ASCE, V. 124, No. 1, 1998, pp. 24-34. doi: 10.1061/(ASCE)0733-9445(1998)124:1(24)
22. Corley, W. G.; Fiorato, A. E.; and Oesterle, R. G., "Structural Walls," *Significant Developments in Engineering Practice and Research*, SP-72, M. A. Sozen, ed., American Concrete Institute, Farmington Hills, MI, 1981, pp. 77-132.
23. Baumann, T., and Rusch, H., "Versuche zum Studium der Verdubelungswirkung der Biegezugbewehrung eines Stahlbetonbalkens," Wilhelm Ernst und Sohn, Berlin, Germany, 1970.
24. He, L., "Shear Behaviour of High-Strength Concrete Beams," *MEng Research Report*, School of Civil and Structural Engineering, Nanyang Technological University, Singapore, 1998.
25. Maeda, Y., "Study on Load-Deflection Characteristics of Reinforced Concrete Shear Walls of High Strength Concrete – Part I Lateral Loading Test (in Japanese)," Research Institute Maeda Construction Corporation, Tokyo, Japan, 1986, pp. 97-107.
26. Okamoto, S., "Study on Reactor Building Structure Using Ultra-High Strength Materials: Part I. Bending Shear Test of RC Shear Wall – Outline," Summaries of Technical Papers of Annual Meeting, Architectural Institute of Japan, Tokyo, Japan, 1990, pp. 1469-1470. (in Japanese)
27. Mo, Y. L., and Chan, J., "Behavior of Reinforced Concrete Framed Shear Walls," *Nuclear Engineering and Design*, V. 166, No. 1, 1996, pp. 55-68. doi: 10.1016/0029-5493(96)01244-7
28. Kabeyasawa, T., and Hiraishi, H., "Tests and Analyses of High-Strength Reinforced Concrete Shear Walls in Japan," *High-Strength Concrete in Seismic Regions*, SP-176, C. W. French and M. E. Kreger, eds., American Concrete Institute, Farmington Hills, MI, 1998, pp. 281-310.
29. Farvashany, F. E.; Foster, S. J.; and Rangan, B. V., "Strength and Deformation of High-Strength Concrete Shearwalls," *ACI Structural Journal*, V. 105, No. 1, Jan.-Feb. 2008, pp. 21-29.
30. Burgueno, R.; Liu, X.; and Hines, E. M., "Web Crushing Capacity of High-Strength Concrete Structural Walls: Experimental Study," *ACI Structural Journal*, V. 111, No. 1, Jan.-Feb. 2014, pp. 37-48.

# aci<sup>®</sup> in Your Classroom

*Integrate aci<sup>®</sup> into your classroom!*

To support future leaders, ACI has launched several initiatives to engage students in the Institute's activities and programs – select programs that may be of interest to Educators are:

- **Free student membership** – encourage students to sign up
- **Special student discounts on ACI 318 Building Code Requirements for Structural Concrete, ACI 530 Building Code Requirements and Specification for Masonry Structure, & Formwork for Concrete manual.**
- **Access to Concrete International** – free to all ACI student members
- **Access to ACI Structural Journal and ACI Materials Journal** – free to all ACI student members
- **Free sustainability resources** – free copies of Sustainable Concrete Guides provided to universities for use in the classroom
- **Student competitions** – participate in ACI's written and/or team-based competitions
- **Scholarships and fellowships** – students who win awards are provided up to \$10,000 and may be offered internships and paid travel to attend ACI's conventions
- **ACI Award for University Student Activities** – receive local and international recognition for your University's participation in concrete related activities
- **Free access to ACI Manual of Concrete Practice** – in conjunction with ACI's chapters, students are provided free access to the online ACI Manual of Concrete Practice
- **ACI online recorded web sessions and continuing education programs** – online learning tools ideal for use as quizzes or in-class study material

## APPENDIX

An example of calculations of RC wall shear strength using the authors' proposed model is given here. A specimen from the authors' experiment [6] is used, i.e. specimen J5.

The procedure is given as follows (in SI unit):

### Specimen J5 data:

Concrete compressive strength,  $f'_c = 103.3$  MPa

Wall gross cross section area,  $A_g = 196000$  mm<sup>2</sup>

Axial load applied at top of wall,  $P = 1012$  kN (compression)

Wall height,  $h_w = 2000$  mm

Wall length,  $l_w = 1000$  mm

Thickness of wall web,  $t_w = 100$  mm

Width of boundary element,  $b_f = 500$  mm

Thickness of boundary element,  $t_f = 120$  mm

Ratio of vertical reinforcement in boundary element,  $\rho_b = 0.0388$

Yield strength of vertical reinforcement in boundary element,  $f_{yb} = 630$  MPa

Ratio of vertical shear (web) reinforcement in wall,  $\rho_v = 0.0028$

Yield strength of vertical shear reinforcement,  $f_{yv} = 610$  MPa

Ratio of horizontal shear (web) reinforcement in wall,  $\rho_h = 0.0028$

Yield strength of horizontal shear reinforcement,  $f_{yh} = 610$  MPa

Experimental wall shear strength,  $V_{exp} = 595.76$  kN

### Calculation of nominal shear strength ( $V_n$ ) according to the proposed model:

1. Calculate  $\sigma_r$  as  $0.02f'_c$  and  $\zeta$  using Eq. (11) assuming  $\varepsilon_r$  equal to 0.005.

$$\sigma_r = 0.02f'_c$$

1  $\sigma_r = 0.02 \times 103.3$

2  $\sigma_r = 2.07 \text{ MPa}$

3  $\zeta = \left( \frac{5.8}{\sqrt{f'_c}} \leq 0.9 \right) \left( \frac{1}{\sqrt{1 + 400\varepsilon_r}} \right)$

4  $\zeta = \left( \frac{5.8}{\sqrt{103.3}} \leq 0.9 \right) \left( \frac{1}{\sqrt{1 + 400 \times 0.005}} \right)$

5  $\zeta = 0.33$

6 2. Check whether both web reinforcements reach their yield strengths or diagonal concrete  
7 strut crushes using Eq. (10).

8  $-\sigma_d > -\sigma_v - \sigma_h + \sigma_r + \rho_v f_v + \rho_h f_h$

9  $-(\zeta f'_c) > -\left(-\frac{P}{A_g}\right) - 0 + \sigma_r + \rho_v 0.8 f_{yv} + \rho_h 0.8 f_{yh}$

10  $(0.33 \times 103.3) > (5.16) - 0 + 2.07 + 0.0028 \times 488 + 0.0028 \times 488$

11  $34.09 > 9.96 \rightarrow$  both web reinforcements reach yield strengths

12  $\sigma_d = -9.96 \text{ MPa}$

13 3. Calculate  $\theta$  using Eq. (12).

14  $\theta = \sin^{-1} \left( \sqrt{\frac{-\sigma_v + \sigma_r + \rho_v f_v}{-\sigma_d + \sigma_r}} \right)$

15  $\theta = \sin^{-1} \left( \sqrt{\frac{5.16 + 2.07 + 0.0028 \times 488}{9.96 + 2.07}} \right)$

16  $\theta = 57.71^\circ$

17 4. Calculate  $D_u$  using Eq. (13).

18  $b_f = 500 \text{ mm} < 0.5 h_w + t_w = 1100 \text{ mm (OK)}$

19  $A_{sb} = \rho_b \times b_f \times t_f$

20  $A_{sb} = 0.0388 \times 500 \times 120$

21  $A_{sb} = 2328 \text{ mm}^2$



1 
$$d_{be} = \sqrt{\frac{A_{sb}}{0.25\pi}}$$

2 
$$d_{be} = \sqrt{\frac{2328}{0.25\pi}}$$

3 
$$d_{be} = 54.44 \text{ mm}$$

4 
$$D_u = 1.64b_{ef}d_{be}\sqrt[3]{f'_c}$$

5 
$$D_u = 1.64 \times (500 - 54.44) \times 54.44 \times \sqrt[3]{103.3}$$

6 
$$D_u = 186.65 \text{ kN}$$

7 5. Calculate  $V_n$  using Eq. (14).

8 
$$V_n = (\sigma_r - \sigma_d) \sin \theta \cos \theta t_w d_w + 1.64b_{ef}d_{be}\sqrt[3]{f'_c}$$

9 
$$V_n = \frac{[(2.07 + 9.96) \sin 57.71^\circ \cos 57.71^\circ \times 100 \times 880]}{1000} + 186.65$$

10 
$$V_n = 478.07 + 186.65$$

11 
$$V_n = 664.72 \text{ kN}$$

12 Thus,  $V_{exp}/V_n = 595.76/664.72 = 0.90$

13